Hydraulic jump in one-dimensional flow

S.B. Singha[1,a], J.K. Bhattacharjee[2,b], and A.K. Ray[3,c]

[1] Department of Theoretical Physics, Tata Institute of Fundamental Research, Homi Bhaba Road, Mumbai 400005, India
[2] Department of Theoretical Physics, Indian Association for the Cultivation of Science, Jadavpur, Kolkata 700032, India
[3] Harish-Chandra Research Institute, Chhatnag Road, Jhunsi, Allahabad 211019, India

Abstract. In the presence of viscosity the hydraulic jump in one dimension is seen to be a first-order transition. A scaling relation for the position of the jump has been determined by applying an averaging technique on the stationary hydrodynamic equations. This gives a linear height profile before the jump, as well as a clear dependence of the magnitude of the jump on the outer boundary condition. The importance of viscosity in the jump formation has been convincingly established, and its physical basis has been understood by a time-dependent analysis of the flow equations. In doing so, a very close correspondence has been revealed between a perturbation equation for the flow rate and the metric of an acoustic white hole. We finally provide experimental support for our heuristically developed theory.

PACS. 47.15.Cb Laminar boundary layers – 47.60.+i Flows in ducts, channels, nozzles, and conduits – 47.32.Ff Separated flows

1 Introduction

A stream of water impinging vertically on to a horizontal surface spreads out radially in a thin sheet along the plane from the point of impingement, and at a certain radius the height of the flowing layer of water suddenly increases. In this two-dimensional flow, such an abrupt increase in the level of the liquid is known as the circular hydraulic jump [1–3]. It is a familiar observation, seen everyday in the kitchen sink. A similarly abrupt increase in the height – a jump – occurs in the one-dimensional flow as well, and this phenomenon finds mention in many introductory text books on hydrodynamics [4–8]. A very regularly cited practical example of the jump in the one-dimensional flow is the passage of a tidal bore up a river [7]. However, the texts include viscosity – arguably the primary physical cause of the jump – only through a phenomenologically added friction term [6]. Consequently, starting from the Navier-Stokes equation, it has not been possible to predict the position of the jump in terms of the volumetric flow rate. For the two-dimensional flow, on the other hand, the role of viscosity has been very clearly taken into account in the works of Bohr et al. [9–11]. This has led to a scaling dependence for the position of the jump on the volumetric flow rate. The two-dimensional problem, however, is sufficiently complicated, and in predicting the position of the jump in this case, knowledge of asymptotic solutions has been necessary to a fair extent.

Motivated by the methods applied to study the two-dimensional flow, and by the results obtained thereof, we make a similar analysis of the one-dimensional flow in this work. We derive a profile of the height of the liquid layer in a one-dimensional open-channel flow by making transparent approximations about the nature of the flow. We find that the position of the jump is sensitive to the vertical profile of the velocity field, and we make use of this dependence to conclude that the profile is far from parabolic and resembles more closely a turbulent profile. There exists no definite result for the magnitude of the jump. Text books [5–8] analyse the problem in one dimension, from which it can be shown that for h_1 and h_2 being the heights of the liquid layer before and after the jump respectively, the ratio h_2/h_1 is unity for the critical value of the Froude number $\mathcal{F}$ (i.e. for $\mathcal{F} = 1$), and increases smoothly as the Froude number is increased from unity. This indicates that the jump is a second-order transition. Contradicting this viewpoint, in our present analysis we put forward a heuristic picture of the role of viscosity and find that in its presence the jump attains a finite value at the critical Froude number. This is exactly what happens in a first-order transition. In our calculations we also establish a connection between the magnitude of the jump and the outer boundary condition. We use steady hydrodynamic equations to obtain the position and the height of the jump. In the process we reinforce our conclusion that the jump is of the nature of a first-order transition.

[a] e-mail: sbsingha@theory.tifr.res.in
[b] e-mail: tpjkb@mahendra.iacs.res.in
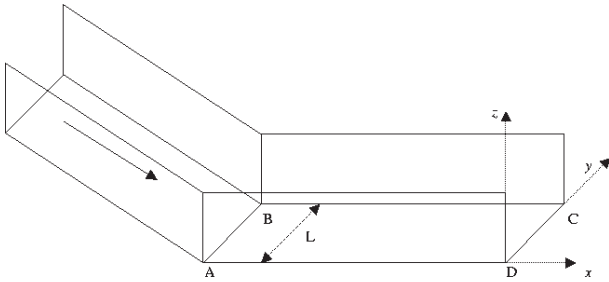[c] e-mail: arnab@mri.ernet.in

Fig. 1. The geometry of the experimental set up. The horizontal flow starts from the edge AB.

Furthermore, we carry out a time-dependent linearised perturbative analysis about the steady flow solution. We perturb the steady and constant flow rate, and see that viscous dissipation, of course, drives the system back towards stability, but what we have made a note of with much greater interest is that the equation for perturbation in the flow has a remarkable degree of closeness with a metric that implies an acoustic white hole. This analogy, coupled with some characteristic time scales obtained through the perturbative analysis, enables us to argue for a physical basis behind the formation of the jump.

It is in a largely heuristic spirit that we have made our theoretical foray into the channel flow problem. To bolster our arguments, we have therefore brought forth some experimental evidence in support of our theory. We have measured the magnitude of the jump and the height profile of the flow before the jump. On both counts we find good agreement with our theory. From our experimental data we can also easily infer that the parabolic profile in the vertical direction has no validity.

2 Role of viscosity: a heuristic study

The flow occurs in a channel of width L, with L being very much greater than the depth of the liquid layer, as has been schematically shown in Figure 1. At some point the depth changes from h_1 to h_2. We work with a control volume which extends from a point before the jump to a point after the occurrence of the jump. Ignoring the effect of viscosity, the continuity equation can be written down as

$$Lh_1 u_1 = Lh_2 u_2 = Q \qquad (1)$$

in which u_1 and u_2 are the flow velocities before and after the jump respectively, while Q is the volumetric flow rate. The momentum change $\rho Q (u_2 - u_1)$ per unit time is brought about by the force due to the pressure difference. This gives the balancing condition

$$\frac{1}{2}\rho g L \left(h_1^2 - h_2^2 \right) = \rho Q \left(u_2 - u_1 \right). \qquad (2)$$

First writing $\mathcal{H} = h_2/h_1$ and the Froude number $\mathcal{F}$ as $\mathcal{F} = u_1^2/gh_1$, we combine equations (1) and (2), to get

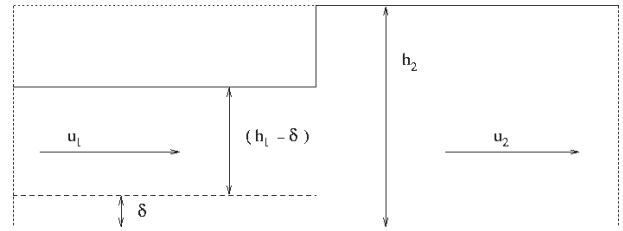$$\mathcal{H}\left(1 + \mathcal{H}\right) - 2\mathcal{F} = 0 \qquad (3)$$

Fig. 2. Control volume of the flow, demarcated by the dotted lines. The boundary layer has an average thickness of δ.

which can be solved to get $2\mathcal{H} = -1 + \sqrt{1 + 8\mathcal{F}}$. If we now write $\mathcal{F} = 1 + \vartheta$ with the condition $0 < \vartheta \ll 1$, then to first order in ϑ we will get $\mathcal{H} = 1 + 2\vartheta/3$, which establishes the standard text book interpretation [5–7] of the jump being a continuous transition as a function of $\mathcal{F}$.

We need to modify the above picture in the presence of viscosity. The most important contribution of viscosity will be the formation of a boundary layer. Practically speaking, the thickness of the boundary layer increases as the flow progresses along the plane, but in our control volume we have constrained the flow to have an average thickness of δ, within which the velocity increases from zero to u_1, while over the depth of $h_1 - \delta$, the flow velocity remains at a constant value of u_1. This state of affairs has been schematically represented in Figure 2. After the jump, beyond a mixing zone characterized by vortices, the flow has a mean speed u_2 and an increased depth h_2. However, it must be noted here that following the jump, the flow has been known to be turbulent – something that may very readily be appreciated from the analogous case of the circular hydraulic jump [12] – and it becomes too much complicated to be thought of simply in terms of a boundary layer. Therefore we keep our analysis of the control volume confined to the flow region before the jump. Within the boundary layer we make use of an arbitrary profile i.e. $u(z) = u_1\varphi(z/\delta)$ with $\varphi(\xi) \leq 1$ for all ξ, and with ξ itself constrained by the range $0 \leq \xi \leq 1$. The continuity equation now reads

$$Lu_1 \left(h_1 - \delta \right) + L \int_0^\delta u_1 \varphi\left(\frac{z}{\delta} \right) \mathrm{d}z = Lu_2 h_2 = Q \qquad (4)$$

which, following some manipulations, can be rendered as

$$Lu_1 \left[h_1 - \delta \left(1 - I_1 \right) \right] = Lu_2 h_2 = Q \qquad (5)$$

where $I_1 = \int_0^1 \varphi(\xi)\,\mathrm{d}\xi$. In the presence of viscosity, this is the modified form of equation (1).

The force balance equation requires a similar modification in the momentum flow rate. Before the jump the amount of momentum entering the control volume per unit time is

$$L\rho \left(h_1 - \delta \right) u_1^2 + L\rho \int_0^\delta u_1^2 \varphi^2\left(\frac{z}{\delta} \right) \mathrm{d}z =$$
$$\rho Q u_1 - L\rho u_1^2 \delta \left(I_1 - I_2 \right) \quad (6)$$

where $I_2 = \int_0^1 \varphi^2(\xi)\,\mathrm{d}\xi$. The amount of momentum leaving the control volume per unit time is $\rho Q u_2$ and the force

due to pressure on the control volume is $\rho L g \left(h_1^2 - h_2^2\right)/2$ acting to the right. The force balance equation now becomes,

$$\rho Q \left(u_2 - u_1\right) + L\rho\delta u_1^2 \left(I_1 - I_2\right) = \frac{1}{2}\rho g L \left(h_1^2 - h_2^2\right). \quad (7)$$

Using the continuity condition as expressed in equation (5), we find

$$u_1^2 \left[h_1 - \delta(1 - I_1)\right]\left[\frac{h_1}{h_2} - 1 - \frac{\delta\left(1 - I_1\right)}{h_2}\right]$$
$$+ \delta u_1^2 \left(I_1 - I_2\right) = \frac{g}{2}\left(h_1^2 - h_2^2\right). \quad (8)$$

As we have done for the inviscid case, we use the same definition of $\mathcal{H}$ and $\mathcal{F}$, and obtain an expression from equation (8) that reads as

$$2\mathcal{F}\left(\frac{1}{\mathcal{H}} - 1\right) - 2\mathcal{F}\frac{\delta}{h_1}\left[2\left(1 - I_1\right)\frac{1}{\mathcal{H}} + I_2 - 1\right]$$
$$+ 2\mathcal{F}\frac{\delta^2}{h_1^2}\left(1 - I_1\right)^2\frac{1}{\mathcal{H}} = 1 - \mathcal{H}^2 \quad (9)$$

from which we can easily see that if $\delta = 0$, i.e. if the effect of viscosity is neglected, then the result given by equation (3) will be recovered. In this inviscid limit, prescribing $\mathcal{F} = 1 + \vartheta$ leads to $\mathcal{H} = 1 + \varepsilon$ with $\varepsilon = 2\vartheta/3$. In the presence of viscosity, we once again seek a jump solution by writing $\mathcal{H} = 1 + \varepsilon$ with $\varepsilon > 0$ for $\mathcal{F} = 1 + \vartheta$. In the limit $\vartheta \longrightarrow 0$, we will then have the cubic equation

$$\varepsilon^3 + 3\varepsilon^2 + 2\frac{\delta}{h_1}\left(1 - I_2\right)\left[\varepsilon - \frac{\left(1 + I_2 - 2I_1\right)}{\left(1 - I_2\right)}\right]$$
$$+ 2\frac{\delta^2}{h_1^2}\left(1 - I_1\right)^2 = 0. \quad (10)$$

It is clear that there can be no positive root of ε which is greater than $(1 + I_2 - 2I_1)/(1 - I_2)$ since in that case all terms on the left hand side of equation (10) will be positive. For a Couette profile $I_1 = 1/2$ and $I_2 = 1/3$. This gives $\varepsilon = 0.5$ as an upper limit. For the parabolic profile $I_1 = 2/3$ and $I_2 = 8/15$, giving $\varepsilon = 0.43$ as a maximum value. On the other hand, a continuous transition would imply that $\varepsilon = 0$. If we use this value of ε in equation (10), we will get the condition $\delta/h_1 = (1 + I_2 - 2I_1)/(1 - I_1)^2$, which, for both the Couette and the parabolic profiles should give a value of δ/h_1 to be greater than unity. This is physically an untenable result, because δ is the average thickness of the boundary layer taken in the region before the jump, and as such, its value must be less than h_1. This inconsistency is indication enough that ε is not zero, and therefore the transition is not continuous.

For a more methodical evaluation of the roots of ε, we will have to solve equation (10). To that end, for notational convenience we write the third degree expression on the left-hand side of equation (10) as $\Phi(\varepsilon)$, and then solve for $\Phi(\varepsilon) = 0$. To find the roots of this cubic equation, it would be necessary to eliminate the second degree term in ε, by the suitable substitution $\varepsilon = \zeta - 1$.
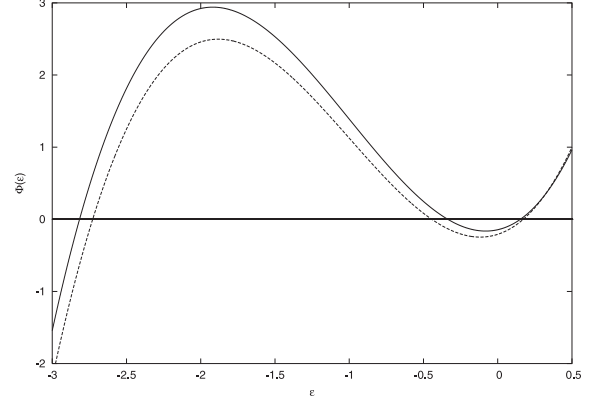

Fig. 3. Plot of $\Phi(\varepsilon)$ versus ε. The roots of ε as given by equation (10), are to be found for $\Phi(\varepsilon) = 0$. Both plots have been drawn for $\delta/h_1 = 0.5$, with the continuous curve representing the parabolic profile, and the dotted curve representing the profile for the Couette flow.

This will then render equation (10) in the standard form as $\zeta^3 + \mathcal{P}\zeta + \mathcal{Q} = 0$, where $\mathcal{P} = -3 + 2(1 - I_2)\delta/h_1$ and $\mathcal{Q} = 2[1 - (1 - I_2)\delta/h_1 + (1 - I_1)^2(\delta/h_1)^2]$. The discriminant, $\mathcal{D}$, is given by $\mathcal{D} = (\mathcal{Q}^2/4) + (\mathcal{P}^3/27)$.

We choose 0.5 as a fiduciary value for δ/h_1, and using this number for both the parabolic profile and the profile for the Couette flow, we find $\mathcal{D} < 0$. This must then imply that there should be three real roots of ε for $\Phi(\varepsilon) = 0$. This is very much in keeping with the fact that the function $\Phi(\varepsilon)$ has two real turning points, which can be obtained from the condition $\Phi'(\varepsilon) = 0$. These points are at $\varepsilon = -1 \pm \sqrt{1 - (2/3)(1 - I_2)\delta/h_1}$. Further, when $\varepsilon = 0$, the function $\Phi(\varepsilon)$ has a negative value. This, in conjunction with the fact that $\Phi(\varepsilon) \longrightarrow +\infty$ when $\varepsilon \longrightarrow +\infty$, could only mean that at most there should be only one positive real root of ε, a conclusion that has been clearly illustrated in Figure 3, in which we have plotted $\Phi(\varepsilon)$ against ε. For both the Couette and the parabolic profiles, three roots are to be found for $\Phi(\varepsilon) = 0$, and in each case only one of these roots is positive. A numerical evaluation by the bisection method shows that for a parabolic profile the positive root of ε is about 0.15, while for the Couette flow it is 0.17. For both these cases we have also assured ourselves that even for the limiting case of δ/h_1 being unity, ϵ will have a positive root. The inescapable conclusion therefore is that the jump is a first-order transition, independent of the vertical velocity profile, because at the critical Froude number ($\mathcal{F} = 1$) the jump has a finite non-zero value. The present analysis drives home the point that when dissipation is included in the conventional control volume analysis, the second-order transition immediately changes to a first-order transition.

3 A hydrodynamic analysis from the steady flow equations

We consider an open rectangular channel of width L (as shown schematically in Fig. 1) in which a liquid is flowing

in streamline motion. An arrangement is made such that the liquid flows down an inclined channel and starts its one dimensional motion in the horizontal plane from the edge AB. The x axis is chosen in the direction of flow, the y axis along the width of the channel and the z axis in the vertical upward direction. At any point, the velocity of the liquid is, in general, a function of the coordinates x, y and z. In our present arrangement the width of the channel is sufficiently large (about 9.1 cm) when compared with the height of the liquid layer (which is of the order of a few millimetres), and we can therefore assume that there is no variation along the y axis for the velocity. On the other hand, both its x component, u, and z component, w, would have a spatial dependence in the form $u \equiv u(x,z)$ and $w \equiv w(x,z)$.

For an incompressible fluid, the local continuity equation gives,

$$\frac{\partial u}{\partial x} + \frac{\partial w}{\partial z} = 0 \qquad (11)$$

and for a not very viscous liquid (e.g. water) the Navier-Stokes equation in the boundary-layer approximation [13] gives

$$u\frac{\partial u}{\partial x} + w\frac{\partial u}{\partial z} = -g\frac{\mathrm{d}h}{\mathrm{d}x} + \nu\frac{\partial^2 u}{\partial z^2} \qquad (12)$$

where $h \equiv h(x)$ is the height of the liquid layer at a distance x, and ν is the kinematic viscosity. The boundary conditions of the flow are $u(x,0) = w(x,0) = 0$, and $\partial u/\partial z = 0$ at $z = h(x)$. In addition to this, the condition for constant volume flux gives

$$L \int_0^{h(x)} u(x,z)\,\mathrm{d}z = Q. \qquad (13)$$

We have assumed here that the shearing stress is zero at the free surface $z = h(x)$, since the viscosity of air is negligible. In the boundary-layer approximation it is assumed that the vertical velocity $w(x,z)$ is very small compared with the horizontal component $u(x,z)$. Furthermore, the variation of $u(x,z)$ is much faster in the z direction as compared with the x direction.

At this stage we follow Bohr et al. [9] to do an averaging of the flow variables over the z direction. We define

$$\langle \psi(x,z) \rangle = \frac{1}{h(x)} \int_0^{h(x)} \psi(x,z)\,\mathrm{d}z \qquad (14)$$

where the averaged quantity in the angled brackets becomes a function of x only. Under the assumption of a flat free surface such that $w(x,z) = 0$ at $z = h(x)$, and along with the use of equation (11), we can readily show that

$$\left\langle w\frac{\partial u}{\partial z} \right\rangle = \left\langle u\frac{\partial u}{\partial x} \right\rangle \qquad (15)$$

and

$$\left\langle \frac{\partial^2 u}{\partial z^2} \right\rangle = -\frac{1}{h(x)}\frac{\partial u}{\partial z}\bigg|_{z=0}. \qquad (16)$$

We now make the approximations,

$$\left\langle u\frac{\partial u}{\partial x} \right\rangle = \alpha\langle u\rangle\frac{\partial\langle u\rangle}{\partial x} \qquad (17)$$

and

$$\frac{\partial u}{\partial z}\bigg|_{z=0} = \beta\frac{\langle u\rangle}{h(x)} \qquad (18)$$

where α and β are numbers of $\mathcal{O}(1)$ and they depend upon the velocity profile. For a parabolic profile $\alpha = 6/5$ and $\beta = 3$. It is easy to check that the parameters α and β are strictly constants when we make, following Watson [3], the reasonable scaling ansatz that $u(x,z) = U(x)F[z/h(x)]$. The fact that our experiment will determine a combination of α and β is important regarding the nature of the vertical profile of the velocity field over which we average.

With the above approximations and identity, and writing $\langle u\rangle$ as v, equation (12) becomes

$$2\alpha v\frac{\mathrm{d}v}{\mathrm{d}x} = -g\frac{\mathrm{d}h}{\mathrm{d}x} - \beta\nu\frac{v}{h^2}. \qquad (19)$$

From equation (13) we get $Lvh = Q$, which we can use to eliminate v from equation (19) and get

$$\left[2\alpha\left(\frac{Q}{L}\right)^2 - gh^3\right]\frac{\mathrm{d}h}{\mathrm{d}x} = \beta\nu\frac{Q}{L}. \qquad (20)$$

The derivation of the above equation may look somewhat heuristic, but it has been much more systematic to the extent that it avoids the inclusion of an artificial friction loss. The structure of this equation, however, is quite similar to what is well known in hydraulic jump literature [6], to derive which, the conventional recourse has been to use the Bernoulli equation supplemented by a friction loss. In our derivation of equation (20), the approximations made on the Navier-Stokes equation have been clearly delineated, and the resulting profile has been seen to be sensitive to the velocity field in a fashion that can be experimentally probed. This equation shows that if $\nu = 0$, then $h(x)$ would be a constant. Therefore, without viscosity the hydraulic jump can be obtained only if we explicitly seek a solution with the jump extraneously imposed, which is the way it has been conventionally treated in text books. The jump occurs when $\mathrm{d}h/\mathrm{d}x$ displays singular behaviour at $h = h_\mathrm{j}$ such that $gh_\mathrm{j}^3 = 2\alpha(Q/L)^2$. The advantage of equation (20) is that it can be exactly integrated. This gives,

$$gh\left(h_\mathrm{j}^3 - \frac{h^3}{4}\right) = \beta\nu\frac{Q}{L}x + \mathcal{C} \qquad (21)$$

where $\mathcal{C}$ is a constant of integration. The position x_j of the jump is obtained by setting $h = h_\mathrm{j}$ in equation (21). This yields

$$x_\mathrm{j} = \frac{3}{\beta}\left(\frac{\alpha^4}{4}\right)^{1/3}\left(\frac{Q}{L}\right)^{5/3}\nu^{-1}g^{-1/3} + \tilde{\mathcal{C}} \qquad (22)$$

where $\tilde{\mathcal{C}}$ is some other constant.

The complete profile of $h(x)$ is described by equation (21), but it should be noted that it gives multiple $h(x)$ for a given x. However, for values of $h(x)$ which are even moderately less that h_j, the profile according to equation (21) can be approximated as

$$h(x) \sim \left(\frac{\beta \nu}{2\alpha} \frac{L}{Q} \right) x \qquad (23)$$

which tells us that for small x the height of the liquid layer increases linearly. This feature is markedly different from the case of the radial spread of a liquid stream on a horizontal plate in which the height gradually decreases in the region within the jump [1].

With the help of equation (21) we are now in a position to get a physical picture of the jump. We introduce the dimensionless variables $H = h/h_j$ and $X = x/\tilde{x}_j$ in which, $\tilde{x}_j = x_j - \tilde{\mathcal{C}}$. We thus obtain a dimensionless form of equation (21) as

$$4H - H^4 = 3\,(X - D) \qquad (24)$$

with D being a dimensionless constant. Differentiating equation (24) will readily show that at $H = 1$, the function $H(X)$ will have a vertical tangent – something that can be conceived of as a discontinuity in the physical flow. Our analysis is restricted to the range $X \geq 0$. The point along the X-axis, where the flow will encounter this discontinuity, will be determined by the inner boundary condition. To show this, we set the condition $H = 0$ at an arbitrary $X = X_{in}$, to get $D = X_{in}$. When $X = 1 + X_{in}$, we will have $H = 1$, which gives us a clear indication that the value of X_{in} will determine the position of the discontinuity.

A generic inner boundary condition is that $H = 0$ at $X = 0$ (ignoring a small initial non-zero value of H at $X = 0$), giving us $X_{in} = D = 0$. The solution corresponding to this particular boundary condition is represented by the lower branch in Figure 4. In the dimensionless notation that we have introduced, this means a profile proceeding from $X = 0$ to $X = 1$ and rising from $H = 0$ to $H = 1$. Since the inner solution diverges infinitely at $X = 1$, the flow has to physically go beyond this point by the fitting of the lower branch to the upper branch in Figure 4, through the discontinuity. We treat this discontinuity as the jump in the flow.

The integration constant D for the upper branch is to be fixed by the outer boundary condition. This is determined by the physical requirement that $H = 1$ (infinite slope) at $X = X_e$, with X_e corresponding to a position slightly left to the edge of the channel where the liquid falls off. We cannot extend the solution to the edge due to singular flow at the outlet. For the outer boundary condition stated above we will get the solution $4H - H^4 = 3\,(X - X_e + 1)$. At the position of the jump, i.e. at $X = 1$, the outer solution will give the magnitude of the jump, H_J, making it evident that H_J has a dependence on X_e. It should be a worthwhile exercise to study this dependence.

The roots of H_J can be determined by solving the biquadratic equation given by $H_J^4 - 4H_J + 3\,(2 - X_e) = 0$.
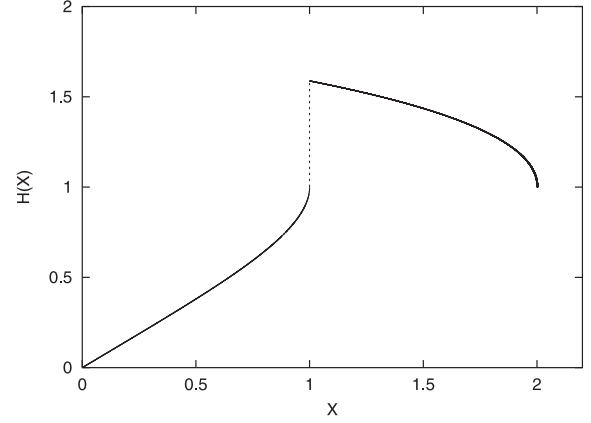

Fig. 4. Fitting the inner and outer solutions via a shock. The inner solution corresponds to $X < 1$, while the outer solution corresponds to $X > 1$. Each solution has been determined by a different boundary condition. The vertical dotted line (the shock) joins the two solutions.

To that end, we will first have to carry out a transformation with the help of a new variable η, to write $\left(H_J^2 + \eta \right)^2 = 2\eta H_J^2 + \eta^2 + 4H_J - 3\,(2 - X_e)$, and then require that by a suitable choice of η, the right hand side will be rendered a perfect square. This requirement will mean that the discriminant of the quadratic in H_J on the right hand side should vanish, to ultimately yield the auxiliary cubic equation $\eta^3 - 3\eta\,(2 - X_e) - 2 = 0$.

The discriminant, Δ, of this cubic equation will be given by $\Delta = 1 - (2 - X_e)^3$, and it is quite easy to see that for $X_e > 1$, there will always be a positive value for Δ. Therefore, η can have only one real root, η_0, given by $\eta_0 = \left(1 + \sqrt{\Delta} \right)^{1/3} + \left(1 - \sqrt{\Delta} \right)^{1/3}$. To solve for H_J, we now use this value of η_0 in the biquadratic equation $\left(H_J^2 + \eta_0 \right) = \pm\sqrt{2\eta_0}\left(H_J + \eta_0^{-1} \right)$. Of course, there will be four roots of H_J, but the real roots should correspond to the choice of the positive sign. Solving the relevant quadratic equation and choosing to keep only the physically meaningful positive root, will give us the solution of H_J as

$$H_J = \sqrt{\frac{\eta_0}{2}} + \sqrt{\left(\frac{2}{\eta_0} \right)^{1/2} - \frac{\eta_0}{2}}. \qquad (25)$$

An interesting conclusion that can be derived from the relation of the jump height above is that for $X_e \gg 1$, the maximum height of the jump will asymptotically be given by $H_J \simeq (3X_e)^{1/4}$.

As a specific case we set $X_e = 2$, and then determining the values of both Δ and η_0, we see that $H_J = 4^{1/3}$. This result could alternatively be derived directly from equation (24) by the use of the boundary condition, $H = 1$, at $X = 2$. This will give $D = 1$, and for this particular boundary condition, the resulting outer solution has been plotted in Figure 4. In this instance the fractional change in height at the jump position would be $4^{1/3} - 1 \simeq 0.59$.

The fitting of the upper and the lower branches (each determined by a different boundary condition) has to be

done via a shock, by requiring that the mass and momentum fluxes remain unchanged through the discontinuity – a condition that may be derived from the inviscid equations. From equations (1) and (2), with both h_1 and h_2 scaled by h_j to give H_1 and H_2, we get what Bohr et al. [9] call the jumpline $H_1 H_2 (H_1 + H_2) = \alpha^{-1}$. The jump takes place when H of the viscous solution in the lower branch of Figure 4 becomes equal to H_1 of the inviscid jumpline for a given value of α. In general, the shock fitting leads to a jump position actually slightly left of $X = 1$.

4 Time-dependence in the channel flow

So far our analysis has been carried out in terms of the steady flow equations only. We now consider explicit time-dependence in both the equation of continuity and the Navier-Stokes equation. This will necessitate the time-dependent generalisation of both the flow variables h, the local height of the flow, and v, the vertically integrated average flow velocity. The resultant dynamic equations may then be written as

$$\frac{\partial h}{\partial t} + \frac{\partial}{\partial x}(vh) = 0 \qquad (26)$$

and

$$\frac{\partial v}{\partial t} + v\frac{\partial v}{\partial x} + g\frac{\partial h}{\partial x} = -\nu\frac{v}{h^2} \qquad (27)$$

respectively.

For the purpose of carrying out a linear stability analysis of the flow in real time, it will be convenient for us to work with a new variable which we define as $f = vh$. The new variable f can be physically associated with the time-dependent volumetric flow rate, and its steady solution, as can be seen from equation (26), is a constant. We use solutions of the form $v(x,t) = v_0(x) + v'(x,t)$ and $h(x,t) = h_0(x) + h'(x,t)$, in which the subscript 0 indicates steady solutions, while the primed quantities are time-dependent perturbations about those steady solutions. Linearising in these fluctuating quantities gives us the fluctuation of f about its constant steady value $f_0 = v_0 h_0 = Q/L$, as

$$f' = v_0 h' + h_0 v'. \qquad (28)$$

In terms of f', we can then write from equation (26),

$$\frac{\partial h'}{\partial t} = -\frac{\partial f'}{\partial x} \qquad (29)$$

and this in turn, along with equation (28), gives,

$$\frac{\partial v'}{\partial t} = \frac{1}{h_0}\left(\frac{\partial f'}{\partial t}\right) + \frac{v_0}{h_0}\left(\frac{\partial f'}{\partial x}\right). \qquad (30)$$

A further partial derivative of equation (30) with respect to time yields

$$\frac{\partial^2 v'}{\partial t^2} = \frac{\partial}{\partial t}\left[\frac{1}{h_0}\left(\frac{\partial f'}{\partial t}\right)\right] + \frac{\partial}{\partial t}\left[\frac{v_0}{h_0}\left(\frac{\partial f'}{\partial x}\right)\right]. \qquad (31)$$

The significance of the form in which we have kept equation (31), will be apparent soon. Linearising in the perturbed quantities in equation (27) gives

$$\frac{\partial v'}{\partial t} + \frac{\partial}{\partial x}(v_0 v') + g\frac{\partial h'}{\partial x} = -\frac{\nu}{h_0^2}\left(v' - 2v_0\frac{h'}{h_0}\right) \qquad (32)$$

which in turn, upon partially differentiating with respect to t, yields

$$\frac{\partial^2 v'}{\partial t^2} + \frac{\partial}{\partial x}\left(v_0\frac{\partial v'}{\partial t}\right) + g\frac{\partial}{\partial x}\left(\frac{\partial h'}{\partial t}\right) = \\ -\frac{\nu}{h_0^2}\left[\frac{\partial v'}{\partial t} - 2\frac{v_0}{h_0}\left(\frac{\partial h'}{\partial t}\right)\right]. \qquad (33)$$

In equation (33) above, we substitute for the first and the second order time derivatives of h' and v' from equations (29) to (31). This will lead to the result

$$\frac{\partial}{\partial t}\left[\frac{1}{h_0}\left(\frac{\partial f'}{\partial t}\right)\right] + \frac{\partial}{\partial t}\left[\frac{v_0}{h_0}\left(\frac{\partial f'}{\partial x}\right)\right] + \frac{\partial}{\partial x}\left[\frac{v_0}{h_0}\left(\frac{\partial f'}{\partial t}\right)\right] \\ + \frac{\partial}{\partial x}\left[\frac{1}{h_0}\left(v_0^2 - gh_0\right)\frac{\partial f'}{\partial x}\right] = -\frac{\nu}{h_0^3}\left(\frac{\partial f'}{\partial t} + 3v_0\frac{\partial f'}{\partial x}\right). \qquad (34)$$

At this juncture it should be most instructive for us to examine equation (34) in its inviscid limit, i.e. when $\nu = 0$. In connection with this, it should also be very much worth our while to consider some recent studies [14–16] which have revealed a close analogy between the propagation of a wave in a moving fluid and of light in curved spacetime. In particular Schützhold and Unruh have shown how gravity waves in a shallow layer of liquid are governed by the same wave equation as a scalar field in curved spacetime [14]. For an inviscid, incompressible and irrotational flow, these authors have prescribed the flow velocity to be the gradient of a scalar potential. Perturbing this potential about its background value, under the restricted condition of the flow height being a constant, leads to an effective metric of the flow, in which the velocity of gravity waves replace the speed of sound in sonic analogs that faithfully reflect features seen in general relativistic studies [14,15].

We now proceed to demonstrate that our perturbative analysis of what is essentially a dissipative system (since it includes viscosity), will, in its inviscid limit, deliver the same metric obtained by Schützhold and Unruh from their purely inviscid model. It must be stressed here that our choice of perturbing the flow rate is particularly expedient, since conservation of matter holds good even in a system that undergoes viscous dissipation. It is to be further noted that the background velocity and flow height in our treatment are in general functions of space and not constants. Having made these observations to emphasise the greater generality and exactitude of our approach, we can then extract the inviscid terms from equation (34) by setting $\nu = 0$, to ultimately render these terms into a compact formulation that looks like [15]

$$\partial_\mu\left(f^{\mu\nu}\partial_\nu f'\right) = 0 \qquad (35)$$

in which, we make the Greek indices run from 0 to 1, with the identification that 0 stands for t and 1 stands

for x. An inspection of the terms in the left hand side of equation (34) – all of them divided by the constant g – will then enable us to construct the symmetric matrix

$$f^{\mu\nu} = \frac{1}{gh_0} \begin{pmatrix} 1 & v_0 \\ v_0 & v_0^2 - gh_0 \end{pmatrix}. \tag{36}$$

Now in terms of the metric $g_{\mu\nu}$, the d'Alembertian for a scalar in curved space, is given by [15]

$$\triangle\psi \equiv \frac{1}{\sqrt{-g}} \partial_\mu \left(\sqrt{-g}\, g^{\mu\nu} \partial_\nu \psi \right) \tag{37}$$

in which $g^{\mu\nu}$ is the inverse of the matrix implied by $g_{\mu\nu}$. Under the equivalence that $f^{\mu\nu} = \sqrt{-g}\, g^{\mu\nu}$, and therefore, $g = \det\left(f^{\mu\nu}\right)$, we can immediately set down an effective metric

$$g_{\text{eff}}^{\mu\nu} = \begin{pmatrix} 1 & v_0 \\ v_0 & v_0^2 - gh_0 \end{pmatrix} \tag{38}$$

that is entirely identical to the one obtained by Schützhold and Unruh, following whom, the inverse effective metric, $g_{\mu\nu}^{\text{eff}}$, can also be easily obtained from equation (38). This shall identify $v_0^2 = gh_0$ as the ergosphere condition on the horizon of either a black hole or a white hole, depending on the direction of the flow. In the case of the two-dimensional circular hydraulic jump, as Volovik has pointed out [16], the jump condition can be closely related to the horizon of a white hole, a surface that nothing can penetrate. This analogy is entirely apt for the channel flow that we are studying here, considering the direction in which the flow proceeds.

Introduction of viscosity in the flow does affect the idealised inviscid conditions in the vicinity of the white hole horizon. Schützhold and Unruh themselves have treated viscosity as a small adjunct effect on the inviscid flow, and have concluded that although viscosity will introduce a thin boundary layer, the flow outside it shall very well be governed by inviscid conditions, and that the basic properties of gravity waves will not be drastically affected. In our presentation of the perturbative analysis, we have systematically included viscosity in our governing equations, which has finally led to equation (34). It is quite evident that the presence of viscosity disrupts the precise symmetry of the inviscid conditions described by equation (35). This obviously implies that the clear-cut horizon condition that one obtains from the inviscid limit, will be affected. However, this effect, for small viscosity, as Schützhold and Unruh have argued, cannot be too drastic. This is very much in conformity with our observation in the previous section that fitting the inner and outer solutions through a shock will shift the position of the jump only slightly. One way or the other, the most important feature to emerge from the analogy of white hole horizon shall remain qualitatively unchanged, namely, that a disturbance propagating upstream from the subcritical flow region (where $v_0^2 < gh_0$) cannot penetrate through the horizon (where $v_0^2 = gh_0$) into the supercritical region of the flow (where $v_0^2 > gh_0$). As we shall see shortly, this property of the flow will have a very crucial bearing on a physical picture

that we shall construct to explain the formation of the hydraulic jump.

For our purposes it should also be important to study the behaviour of the perturbation f'. To that end we go back to equation (34) and recast it in a slightly altered form that looks like

$$\frac{\partial^2 f'}{\partial t^2} + 2\frac{\partial}{\partial x}\left(v_0 \frac{\partial f'}{\partial t}\right) + \frac{1}{v_0}\frac{\partial}{\partial x}\left[v_0\left(v_0^2 - gh_0\right)\frac{\partial f'}{\partial x}\right] = \\ -\frac{\nu}{h_0^2}\left(\frac{\partial f'}{\partial t} + 3v_0 \frac{\partial f'}{\partial x}\right). \tag{39}$$

Using a solution of the type $f'(x,t) = p(x)\exp(-\mathrm{i}\omega t)$ in equation (39) gives an expression that is to be further multiplied by $v_0 p$ throughout, to finally deliver a quadratic equation in ω that is of the form

$$-\omega^2\left(v_0 p^2\right) - \mathrm{i}\omega\left[\frac{\mathrm{d}}{\mathrm{d}x}\left(v_0 p\right)^2 + \nu\frac{v_0 p^2}{h_0^2}\right] \\ + p\frac{\mathrm{d}}{\mathrm{d}x}\left[v_0\left(v_0^2 - gh_0\right)\frac{\mathrm{d}p}{\mathrm{d}x}\right] + 3\nu\frac{v_0^2 p}{h_0^2}\left(\frac{\mathrm{d}p}{\mathrm{d}x}\right) = 0. \tag{40}$$

To have any idea of how the perturbation behaves in time, we treat it as a standing wave. For that purpose we will have to integrate the above equation between two chosen boundaries, at which the perturbation will be constrained to vanish at all times. Between these two boundaries the flow should be continuous. Since we are aware that the jump itself is a discontinuity in the flow, we will have to choose the boundaries to be on one side of the jump only, although equation (40) itself holds true over the entire range of the flow. We have already acquainted ourselves with the fact that a perturbation in the subcritical region will remain confined to this region only. Besides, in this region the flow would have entirely lost its laminar character, and therefore, would be most suited for us to derive some physical insight about the behaviour of the perturbation and the influence of viscosity on that. Therefore, we confine our analysis to the subcritical region of the flow only. As for the boundaries of the perturbation, one of them can be the outer boundary of the steady flow itself, while the inner boundary may be chosen to be very close to the jump. In this regard we treat the jump itself as a boundary wall where all velocity and height fluctuations decay out completely. Under these conditions an integration of equation (40) leads to

$$\omega^2 \int v_0 p^2\,\mathrm{d}x + \mathrm{i}\omega\nu \int \frac{v_0 p^2}{h_0^2}\,\mathrm{d}x - 3\nu \int \left(\frac{v_0}{h_0}\right)^2 p\frac{\mathrm{d}p}{\mathrm{d}x}\,\mathrm{d}x \\ + \int v_0\left(v_0^2 - gh_0\right)\left(\frac{\mathrm{d}p}{\mathrm{d}x}\right)^2\,\mathrm{d}x = 0 \tag{41}$$

which is a result that has been arrived at by carrying out the integration by parts, and then by imposing the requirement that all the integrated "surface" terms vanish at the two boundaries.

Under inviscid conditions, ω will have a purely real solution, and therefore the perturbation will be a standing wave with a constant amplitude in time. However, the

dissipative presence of viscosity will result in the perturbation being damped out, and will restore the system towards a stable configuration. The consequent time-decay of the amplitude of the perturbation will be of the form $\exp(-\nu t/2h_0^2)$. This also gives a time scale for viscous dissipation, which, to an order-of-magnitude, is given by $t_{\mathrm{visc}} \sim h_0^2/\nu$.

It is now important to appreciate that viscous drag in the fluid will also dissipatively slow down the flow on this very same time scale t_{visc}. The information of an advanced layer of fluid slowing down has to propagate upstream to preserve the smooth continuity of the fluid flow. This propagation, however, cannot happen any faster than the speed of the surface gravity waves, $(gh_0)^{1/2}$, and in the region where $v_0 > (gh_0)^{1/2}$, i.e. in the supercritical region, no information therefore can propagate upstream [11]. This is also what we should entirely expect from the modelling of the jump as the horizon of an impenetrable white hole. So a stream of fluid that has arrived later, after having passed through the supercritical region, moves on ahead, yet unhindered and uninformed, till its speed becomes comparable with the speed of the surface gravity waves, and only then does any knowledge about a "barrier" ahead catches up with the fluid. We now define a dynamic time scale, $t_{\mathrm{dyn}} \sim x/v_0$, on which the bulk flow proceeds. If we set $t_{\mathrm{visc}} \simeq t_{\mathrm{dyn}}$ with the additional requirement $v_0 \simeq (gh_0)^{1/2}$, we get the condition for the "news" of the viscous slowing down finally catching up with the bulk flow itself. With the additional constraint that we have from the continuity equation, i.e. $v_0 h_0 = Q/L$, we can then derive a scaling relation for length which is entirely identical to the scaling dependence of the position of the hydraulic jump,

$$x_{\mathrm{j}} \sim \left(\frac{Q}{L}\right)^{5/3} \nu^{-1} g^{-1/3} \qquad (42)$$

as given by equation (22) – a result that we have already obtained from our study of the stationary flow equations.

The crux of the argument that emerges from our analysis is that for the formation of the hydraulic jump, the two time scales, t_{visc} and t_{dyn}, would have to match each other closely when the Froude number, $\mathcal{F}$, is close to unity. Under these conditions, a layer of fluid arriving lately is confronted with a barrier formed by a layer of fluid moving ahead with an abrupt slowness. This slowly moving layer of fluid flowed past earlier in time, and at far distances it has been retarded considerably by viscous drag. Since in this situation there could not be an indefinite accumulation of the fluid, and since continuity of the fluid flow has to be preserved, the newly arrived fluid layer slides over the earlier viscosity dragged slowly moving layer of the fluid, and what we see is a sudden increase in the height of the fluid layer – a hydraulic jump. This gives a conceivable physical basis for understanding how crucial a factor viscosity is behind the formation of the jump, and in connection with this physical picture, it is also worthwhile to ponder the possibility that the viscosity-induced boundary layer of the flow gradually increases in thickness and the jump occurs at that distance, where the boundary layer pervades the entire height of the thin layer of the flowing fluid, i.e. from $z = 0$ to $z = h(x)$.

While dwelling on the issue of the physical picture of the jump formation, we are tempted to adduce a related astrophysical analogy: the formation of hot spots in galaxies. Gaseous jets emanating from galaxies encounter resistance from the intergalactic medium. As a result the tip of the jet is slowed down in comparison with its bulk. This causes energy to accumulate at the tip, and this is a likely explanation for the formation of a hot spot. The gas flow in the jet proceeds at supersonic speeds, but on coming close to the hot spot, the flow experiences an abrupt deceleration. The information of this sudden braking is not conveyed upstream, since no sound wave can move against the supersonic flow. This causes a shock wave to form across the jet [17]. In this particular astrophysical picture, one might discern much similarity of principle with our physical arguments behind the formation of the hydraulic jump in the channel flow.

Another significant point of which we should like to make mention is that instead of equation (27) we could have chosen to use the dynamic generalisation of equation (19) with the dimensionless constants α and β included, but to derive the particular form of the perturbation equation as given by equation (34), we would have to set $\alpha = 1/2$. This argument possibly has an important bearing on the issue of the velocity profile of the flow.

5 Experimental results

A relatively simple experiment, using water, was carried out to substantiate our theoretical propositions. Our objectives were two-fold. First, to verify the linear growth of the surface height of the flow at small distances, and secondly, to verify the scaling of the jump position as given by equation (42). It has been satisfying to note that our theory – presented heuristically in parts – has very much been borne out within the limited objectives of our experiment.

The experimental apparatus has already been illustrated schematically in Figure 1. The water flows in a streamline motion through an open rectangular channel of width L. An arrangement has been made such that the water will flow down an inclined channel, with an inclination of $60°$, and then from the edge AB, will start its one-dimensional motion in the horizontal channel whose length is $70\,\mathrm{cm}$ and width is $9.1\,\mathrm{cm}$. A rectangular box is attached to the base of the inclined channel. Water comes from a tap to the rectangular box. There is a slit in the box through which water flows down the channel. The purpose of the inclined channel is to make the flow laminar from the beginning of the horizontal channel. Although this will introduce a small horizontal component to the flow, in so far as we would be interested in the scaling relations only, any small extraneous addition to the flow should not too drastically affect our observations. In any case, preserving the laminarity of the flow should be necessary for the unambiguous recording of data. For that purpose, the height
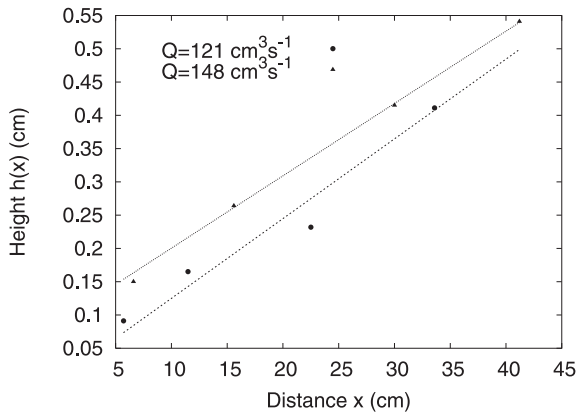
Fig. 5. The height profile $h(x)$ before the jump for different values of Q, the volumetric flow rate.
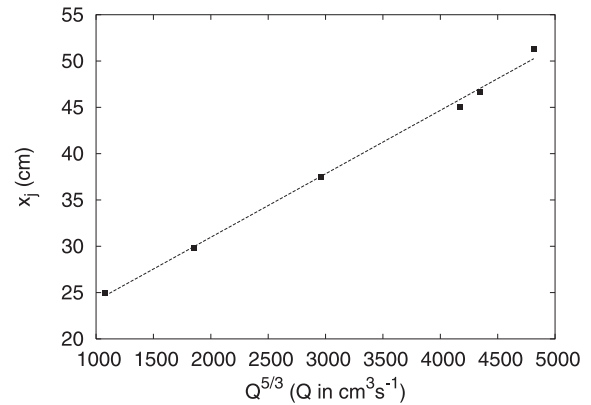

Fig. 6. The position x_j of the jump for different volumetric flow rates Q.

of the water layer has been measured with a travelling microscope. The flow has been viewed through the transparent perspec wall of the horizontal channel. At each value of x, we noted down the vertical positions of the bottom of the flow in contact with the bed of the channel, and of the free surface of the flowing water (both of which were easily identifiable in the field of view of the microscope). The difference of the two readings gave $h(x)$.

Viewed from the top of the channel, the jump itself has been seen to present a curved front across the width (i.e. along the y axis) of the channel. This is because the flow in contact with the boundary walls of the channel (at $y = 0$ and $y = L$ respectively) has been dragged down by viscosity. The position of the jump, x_j, is actually an average value measured over this lateral curved profile.

To estimate the volumetric flow rate, we adopted the simple recourse of collecting the water falling off at the outer edge of the channel, and then of measuring the volume of the water collected for various intervals of time. The average of all these readings has been taken to determine Q. The steadiness of the flow has also been confirmed by this approach. Values of X_e, at the outer edge of the channel (discussed in Sect. 3), range between 1.5 and 2.8 in our experimental set-up.

We observed a very slow rise in $h(x)$ for a while and then a major jump. That the rising profile of $h(x)$ will be linear, as we might rightly expect on the basis of equation (23), has been shown in Figure 5 for two different values of Q. We also show the scaling dependence of the jump position x_j on $Q^{5/3}$ in Figure 6. The predicted linearity from equation (42) has been depicted quite clearly here. It is obvious that once the $5/3$ power dependence of x_j on Q has been established experimentally, the dependence on ν and g, as equation (42) shows, must follow even on the basis of elementary dimensional considerations. So our theoretical scaling law stands vindicated by our simple experiment.

More to this point, we also furnish two photographs of the cross-section of the flow with the jump included. We show a long distance snapshot of the flow in Figure 7. The flow has been dyed red to make it more prominent, when viewed through the transparent perspec wall. The
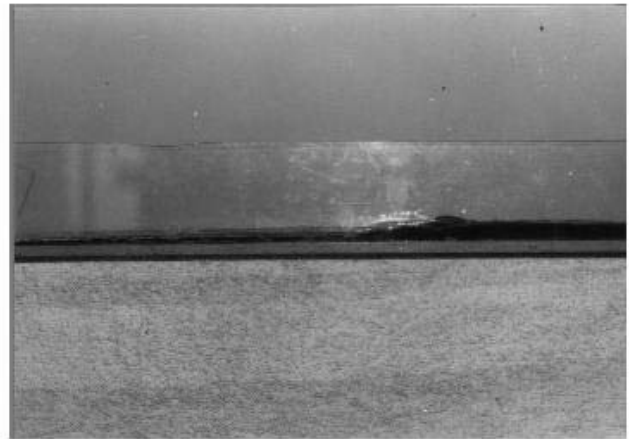

Fig. 7. A sideview of jump region with the flow proceeding from the left to the right. The flow appears black in the photograph, because it has been coloured with a red dye. The jump is clearly discernable, as also are the growth and decay profiles of the surface height, before and after the jump, respectively.

jump is very much discernable in this photograph, but we must also draw attention to the slow linearised growth of the height of the flow much before the jump, followed by its much more rapid growth immediately in front of the jump. This is further followed by a small decrease in the flow level in the region beyond the jump. Qualitatively this is what we should expect on the basis of the plot in Figure 4. That the variation of the flow height we see in the photograph, is not as pronounced as Figure 4 would impress upon us, is because of the fact that the axes in Figure 4 have been scaled in terms of the flow constants, while the variation of the flow height in the actual photograph proceeds on the scale of CGS units. The jump appears much more prominently in the close-up view of the jump region, shown in Figure 8.

From Table 1 it is seen that the jump remains almost constant within an experimental error of about 6%. The combined effect of the theoretical analysis and the experimental results leads us to believe that the magnitude of

Fig. 8. A close-up sideview of the jump region.

Table 1. The magnitude of the jump ε, at different volumetric flow rates Q.

Q ($\mathrm{cm^3 s^{-1}}$)	h_1 (cm)	h_2 (cm)	$\varepsilon = \mathcal{H} - 1$
66	0.415	0.590	0.42
91	0.430	0.619	0.44
121	0.445	0.648	0.46
148	0.573	0.856	0.49
152	0.590	0.890	0.51
162	0.621	0.940	0.51

the jump in a shallow layer flow will show no drastic variation.

The z profile of the velocity field $u(x, z)$ also calls for some comments. The slope in equation (22) depends on the numbers α and β according to the combination $\alpha^{4/3}/\beta$, which, for a parabolic profile ($\alpha = 6/5$ and $\beta = 3$) is about 0.425. This ultimately gives a theoretical estimate of the slope to be approximately 0.204. But the experimental data as plotted in Figure 6 show that the actual slope (nearly 0.007) is much smaller. This leads us to infer that the profile is much steeper than parabolic near the plate and much flatter near the free surface.

In the experiment we have also seen that the flow becomes turbulent after the jump, with the formation of vortices. We have not made any measurement for this region as we have been interested in the laminar flow only. However, we have noticed that for low volumetric flow rates, turbulence in the subcritical flow region dies down appreciably, as the flow proceeds downstream. On the other hand, for high flow rates, turbulence is seen to be sustained right up to the outer boundary of the flow. Qualitatively this is what it should be. Turbulent fluctuations derive their energy from the mean flow. If the mean flow is more energetic, such as it should be for higher flow rates, then turbulent effects will linger in the flow that much longer. Regarding this issue, it should be possible for us, at least in an order-of-magnitude sense, to make a theoretical estimate of the Reynolds number of the turbulent flow, immediately after the jump. In the shallow layer flow,

the largest possible turbulent eddies should have a characteristic length scale that should at most be of the order of the flow height h, in the subcritical region. The characteristic turnover velocity of the eddies should likewise be of the order of (but less than) the velocity of surface gravity waves, $(gh)^{1/2}$. The Reynolds number of the flow, $\mathcal{R}_\mathrm{e}$, should therefore be given by $\mathcal{R}_\mathrm{e} \sim \nu^{-1}(gh^3)^{1/2}$. In our experiment, typical values of the flow constants g and ν would be $1000 \ \mathrm{cm\,s^{-2}}$ and $10^{-2} \ \mathrm{cm^2\,s^{-1}}$, respectively. From Table 1, for various values of Q, we may have an estimate of the characteristic values of the flow height h immediately after the jump. These measurements should then typically give $\mathcal{R}_\mathrm{e} \sim 1000$, an estimate, whose direct verification, however, would be beyond the scope of our experiment.

References

1. R.G. Olsson, E.T. Turkdogan, Nature **211**, 813 (1966)
2. I. Tani, J. Phys. Soc. Jpn **4**, 212 (1949)
3. E.J. Watson, J. Fluid Mech. **20**, 481 (1964)
4. C. Walshaw, D.A. Jobson, *Mechanics of Fluids* (Longman, London, 1979)
5. L.D. Landau, E.M. Lifshitz, *Course of Theoretical Physics – Fluid Mechanics* (Butterworth-Heinemann, Oxford, 1987)
6. S. Granger, *Engineering Fluid Mechanics* (Dover, New York, 1987)
7. T.E. Faber, *Fluid Dynamics for Physicists* (Cambridge University Press, Cambridge, 1995)
8. E. Guyon, J.-P. Hulin, L. Petit, C.D. Mitescu, *Physical Hydrodynamics* (Oxford University Press, Oxford, 2001)
9. T. Bohr, P. Dimon, V. Putkaradze, J. Fluid Mech. **254**, 635 (1993)
10. T. Bohr, C. Ellegaard, A. Espe Hansen, A. Hanning, Physica B **228**, 1 (1996)
11. T. Bohr, V. Putkaradze, S. Watanabe, Phys. Rev. Lett. **79**, 1038 (1997)
12. S.H. Hansen, S. Hørlück, D. Zauner, P. Dimon, C. Ellegaard, S.C. Creagh, Phys. Rev. E **55**, 7048 (1997)
13. H. Schlichting, K. Gersten, *Boundary Layer Theory* (Springer-Verlag, Berlin/Heidelberg, 2000)
14. R. Schützhold, W. Unruh, Phys. Rev. D **66**, 044019 (2002)
15. C. Barceló, S. Liberati, M. Visser, *Analogue Gravity*, e-print: `arXiv:gr-qc/0505065`
16. G.E. Volovik, *The Hydraulic Jump as a White Hole*, e-print: `arXiv:physics/0508215`
17. M.C. Begelman, M.J. Rees, *Gravity's Fatal Attraction: Black Holes in the Universe* (Scientific American Library, New York, 1995)